designs

MDPI

Article

Optimization of Non-Newtonian Flow through a Coat-Hanger Die Using the Adjoint Method

Dastan Igali [1], Omonini Clifford [1], Asma Perveen [1], Dichuan Zhang [2] and Dongming Wei [3,*]

[1] Department of Mechanical and Aerospace Engineering, School of Engineering and Digital Sciences, Nazarbayev University, Kabanbay Batyr Avenue 53, Astana 010000, Kazakhstan; dastan.igali@nu.edu.kz (D.I.); clifford.omonini@nu.edu.kz (O.C.); asma.perveen@nu.edu.kz (A.P.)
[2] Department of Civil and Environmental Engineering, School of Engineering and Digital Sciences, Nazarbayev University, Kabanbay Batyr Avenue 53, Astana 010000, Kazakhstan; dichuan.zhang@nu.edu.kz
[3] Department of Mathematics, School of Sciences and Humanities, Nazarbayev University, Kabanbay Batyr Avenue 53, Astana 010000, Kazakhstan
* Correspondence: dongming.wei@nu.edu.kz

Abstract: The use of coat-hanger dies is prevalent in the plastic film and sheet extrusion industry. The product quality and the power of the extrusion machine depend on the uniformities of the fluid velocity at the exit and the pressure drop. Die manufacturers face the challenge of producing coat-hanger dies that can extrude materials uniformly and with a minimal pressure drop. Previous studies have analyzed the die outlet's flow homogeneity and pressure drop using various numerical simulations. However, the combination of the scheme programming language together with the Adjoint Method of Optimization has yet to be attempted. The adjoint optimization method has been demonstrated to be beneficial in addressing issues related to shape optimization problems and it may also be beneficial in optimizing the design of dies used in polymer melt extrusion. In this study, the proposed innovations involve incorporating both the Scheme programming language and Adjoint solver to examine and optimize the coat hanger's flow homogeneity and pressure drop. Before optimization, the outlet velocity was almost 10 times higher at the die center than at the edges but after optimization, it became more uniform. The proposed optimized coat-hanger die geometry results in more uniform melt flow as demonstrated by the velocity contour plot and the outlet velocity graph in the die slit area, reducing the deviation value from 0.097 to 0.015. Additionally, the mass flux variance across the die outlet decreased by 71.6% from 0.015069 kg m^{-2} s^{-1} to 0.004281 kg m^{-2} s^{-1}. Therefore, using this method reduces the amount of time wasted on trial and error or other optimization techniques that may be limited by design constraints.

Keywords: polymer extrusion; coat-hanger die; adjoint optimization method; Carreau–Yasuda model; non-Newtonian fluid

check for updates

Citation: Igali, D.; Clifford, O.; Perveen, A.; Zhang, D.; Wei, D. Optimization of Non-Newtonian Flow through a Coat-Hanger Die Using the Adjoint Method. *Designs* **2023**, *7*, 138. https://doi.org/10.3390/designs7060138

Academic Editor: Joshua M. Pearce

Received: 24 September 2023
Revised: 30 October 2023
Accepted: 31 October 2023
Published: 1 December 2023

Copyright: © 2023 by the authors. Licensee MDPI, Basel, Switzerland. This article is an open access article distributed under the terms and conditions of the Creative Commons Attribution (CC BY) license (https://creativecommons.org/licenses/by/4.0/).

1. Introduction

The extrusion of polymer sheets and films is widely utilized in the polymer processing industry. Coat-hanger dies are commonly employed in this process [1–3]. For several years, achieving uniform outlet velocity and low-pressure drop has been the primary focus in designing coat-hanger dies [3–5]. When designing dies for polymer extrusion, it is common practice to make changes to the die shape through a process of trial and error to obtain uniform flow at the exit. If the flow channel in a flat die is not built appropriately, the velocity at the exit of the flat die may not be uniform [6]. This results in a variation in the polymer melt thickness over the width of the die.

In many cases, the number of involved variables and the relationships between them limit any optimization according to the trial-and-error corrections. This is because the number of evaluations that are required may become quite high. The adjoint method provides an approach to optimizing shapes that is both more flexible and quicker, regardless

of the number of sensitivities that are being considered. Studies by Han and Wang [3] and Lebaal et al. [6] have shown that non-uniform outlet velocity can result in thickness variation in the final product, while high-pressure drops can lead to increased energy consumption and separation of the die plates [5,7].

The modern die design process relies heavily on optimization techniques [8], with computational fluid dynamics (CFD) being a popular tool due to the increased computational power. Automatic modeling tools have been developed using CFD-based optimization strategies specifically for die applications [2–7,9]. Stochastic methods, such as evolutionary algorithms, are often used with CFD-based geometry optimization techniques to reduce the overall computation cost and find the optimal shape. Genetic algorithms (GA) combined with proxy models are commonly used in these strategies [10].

However, when numerous design variables govern the geometry, the cost of the optimization process can become prohibitively high. Therefore, it is necessary to reduce the design space and solutions effectively [11]. Additionally, due to mechanical and geometrical constraints, improving the performance of practical coat-hanger dies by optimizing existing geometric shapes is often possible. As a result, the optimal design should involve only minor geometry adjustments and closely resemble the initial configuration. In such cases, gradient-based design solutions using adjoint methods can significantly reduce computational costs [11]. Hence, the adjoint method is a practical and efficient option for optimizing the existing coat-hanger die. The benefits of using the adjoint method for enhancing coat-hanger die performance are enticing. Also, executing GAs is much more challenging than most other applications due to the large number of computational resources required for carrying out precise polymer CFD simulations with many design variables.

Several approaches have been suggested to optimize the flow uniformity and pressure drop of coat-hanger die geometries [2–7,9,12,13]. Although the adjoint solver is widely used in aerospace engineering and the automotive industry to address turbulent flow problems, it has seen less adoption in Ansys Fluent for optimizing coat-hanger die designs that account for non-Newtonian fluids [11,14,15]. This approach is attractive for intricate shapes because it is not reliant on the quantity of design factors and consequently demands less computational resources [11]. The cost of using the adjoint method in computation is almost the same as solving the flow equations [16].

The main proposed innovations of this study are the combination of the Scheme programming language and Adjoint solver in the shape optimization of a coat-hanger die design. The results obtained in this study can be employed in various industries for shape optimization of various designs. This helps in the reduction in time wastage in undergoing trial and error or using other optimization techniques, which take so much/are limited by design constraints.

2. Literature Review

Adjoint sensitivity analysis originated in the control theory [17] and has spread to fluid mechanics [17,18]. Subsequently, the method has been used to optimize fluid problems involving shape and topology, particularly when several degrees of freedom exist [19,20]. The adjoint method has also been used in extrusion for various optimization purposes [4,21–28]. Regardless of the number of design parameters provided, the adjoint technique requires only two flow simulations, one for the primal and one for the adjoint system. This approach gives a competitive advantage over standard parametric optimizations of geometry that requires as many flow solutions as parameter combinations. This advantage, particularly regarding big application scenarios and adjoint-based optimization techniques, has made it a vital optimization tool in industries [29,30].

In the case of the application of CFD optimization techniques to the Euler and Navier–Stokes equations for design purposes, adjoint equations are widely used [17–20,31]. With adjoint approaches, computing sensitivity derivatives of a function only requires one flow calculation and one adjoint calculation per given number of design variables. This makes the cost of computation essentially independent of the number of design variables. There

are two formulations of the method: discrete and continuous. In the discrete method, the governing equations are linearized and then discretized. On the other hand, the continuous approach linearizes and then discretizes the equations as well, but allows for more adaptability in discretization, resulting in lower memory and CPU expenses [17]. Discontinuous action in the discretization scheme can be addressed using the continuous approach [29,30]. Nevertheless, using the discrete adjoint method can ensure the accuracy of the final gradients of the adjoint solution by generating the exact sensitivity derivatives of the initial discretization of the governing equations [18]. The process for implementing the discrete adjoint technique is straightforward. It involves linearizing the discretized governing equations in either the primal or tangent problem, creating the tangent problem for sensitivity derivatives. To obtain the discrete adjoint formulation, one must work backwards through the tangent problem and transpose each matrix created along the way. Deriving the tangent problem for boundary conditions is less complex than deriving the adjoint problem. Linearization is often necessary to develop an implicit solution scheme, which aids in finding a solution [31].

Many approaches to adjoint problems center on creating and addressing the adjoint problem for the governing flow equations. However, it is important to note that design optimization involves more than just solving for flow solutions. It also includes dealing with surface and interior mesh deformation. Simplified formulations (especially for structured grids) [17], finite differencing [32], or forward linearization [18] can reduce the sensitivities from additional processes like surface deformation and interior mesh deformation [31].

In this study, a new approach to optimize polymer flow using Ansys Fluent's adjoint solver technique is presented. The main focus is on die design optimization for non-Newtonian fluids, an area with limited studies on the application of this technique. The effectiveness of the adjoint solver in improving melt flow through the die is evaluated through numerical results and contour plots. The research provides a fresh perspective in the field of polymer flow optimization. The Carreau–Yasuda viscosity model is used to model the flow of the polymer melt, and the results are presented through contour plots and graphs that compare the initial and optimized coat-hanger die geometries.

Scheme Programming Language

Scheme is a concise and sophisticated programming language that originated in the 1970s and is based on the Lisp family. The language is renowned for its simplicity, utilizing a clear and uncomplicated syntax, distinguished by the extensive utilization of S-expressions. This programming language prioritizes mathematical functions and utilizes dynamic typing, allowing for adaptable and creative code [33].

Scheme stands out for its use of lexical scoping, which provides clear and predictable variable management. Garbage collection automates memory management, hence, minimizing the likelihood of memory-related failures. Scheme provides a wide range of advanced constructs, such as closures and macros that enhance the production of compact and elegant code.

In addition to its practical applications in software development, Scheme has played a substantial role in the fields of education and research. Its simplicity makes it a good choice for beginners, which is why it is widely used for teaching programming principles. The lasting importance of Scheme in the world of programming and computer science is attributed to its interactive development environment and its ability to be used across multiple platforms [33].

3. Coat-Hanger Die Design

The quality of die design is investigated in this study with regards to how pressure drop and variation in die exit velocity impact it. The dimensions of the extruder and required power are determined by the pressure drop, whereas the thickness uniformity

of the sheet is influenced by the fluctuation in outlet velocity [4,31]. Mathematically, die design optimization is as follows:

$$\min\left(\phi \epsilon \mathcal{R}^N\right) \qquad f(\phi) = P_{in} \tag{1}$$

Such that:

$$g_1(\phi) = \frac{1}{L}\int \left(\frac{\overline{v}(\phi)}{v_a(\phi)} - 1\right)^2 dx \leq \varepsilon_1 \tag{2}$$

Equation (2) is integrated from the edge of the die exit (l_{exit}).

$$g_2(\phi) = \left(\frac{v_a(\phi)}{\overline{v}_p(\phi)} - 1\right)^2 \leq \varepsilon_2 \tag{3}$$

$$g_3{}^k(\phi) = \frac{\| \bigtriangledown h^k(\phi)\|}{\| \bigtriangledown h_p\|} - 1 \leq 0 \tag{4}$$

This nonlinear restricted optimization aims to reduce the inlet pressures P_{in} as much as possible [34].

The constraint g_1 in Equation (2) estimates changes in outlet velocity, which is utilized to achieve an outlet velocity that does not fluctuate while remaining in the range of one [4]. We have this restriction in order to ensure that the mean gap-wise velocity at the outlet $\overline{v}(\phi)$, which is normal to the die outlet in Figure 1, stays close to the average gap-wise exit velocity, $v_a(\phi)$, which is specified as follows:

$$v_a(\phi) = \frac{1}{L}\int_{l_{exit}} \overline{v} dx \tag{5}$$

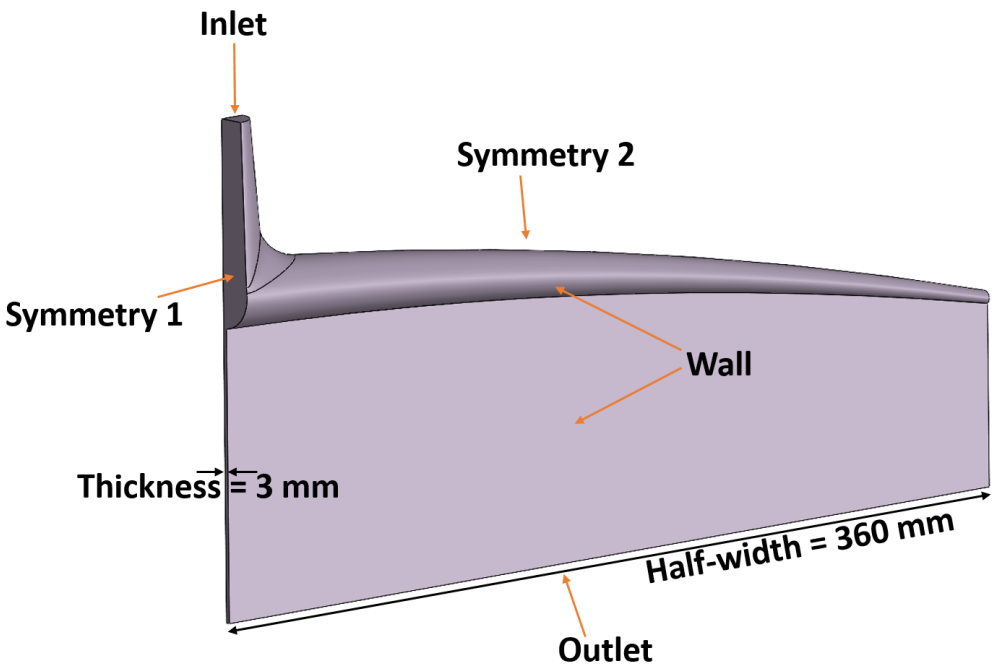

Figure 1. The quarter fluid domain of the coat-hanger die.

The needed overall flow rate Q at which the die is operating is given by [4,31];

$$Q = 2h_{exit}\int_{l_{exit}} \overline{v}_p dx \tag{6}$$

The objective function $f(\phi)$ and constraint ${g_3}^k$ (ϕ) rely directly on the design variables, whereas the constraints g_1 (ϕ) and g_2 (ϕ) rely indirectly on the design variables via the governing equations [4].

3.1. Adjoint-Based Optimization

The effectiveness of adjoint-based optimization for problems with many design variables has been known for some time [4]. By utilizing the adjoint technique, it becomes possible to perform highly precise calculations of sensitivities, i.e., the objective function's derivative with respect to the design parameters. Only one solution of the adjoint equivalents of the governing equation system, in this case the Navier–Stokes equations, is required, which means that the processing effort remains consistent regardless of the number of design variables. Sensitivity analysis can be used to generate information, such as uniform velocity and pressure drop, and is applicable to either a surface mesh representation or a volume mesh of the area that needs improvement [4].

3.2. Design Sensitivity Analysis (DSA)

In order to quickly calculate better designs, gradient-based optimization algorithms take advantage of design sensitivity. The design variables, such as the ½ height of die cavity or inlet pressure variables in ϕ, and performance metrics of the system, such as f, g_1, g_2, and ${g_3}^k$ in Equation (1), are quantified by design sensitivities [4]. Similar to how the flow solution was assessed, equations were developed for the design sensitivities and evaluated them using the FEA. This method of analysis sidesteps the usual mistakes and inefficiencies of FDM.

3.3. DSA for Coat-Hanger Die

Calculating design sensitivity is easy since both the objective function $f(\phi)$ and the constraint ${g_3}^k$ (ϕ) in Equation (1) are established directly on ϕ [4]. The sensitivity analysis for the objective function $f(\phi)$ in Equation (1) can be calculated using the following:

$$\frac{Df(\phi)}{\phi_i} = 1 \; for \; \phi_i = P_{in}, \; otherwise = 0 \tag{7}$$

Using a similar approach, the sensitivity for the constraint ${g_3}^k$ is as follows:

$$\frac{Dg_3^k(\phi)}{D(\phi_i)} = 0 \; for \; \phi_i = P_{in}, \; otherwise = \frac{1}{\| \bigtriangledown h \| \| \bigtriangledown h_p \|} \tag{8}$$

where the gradients of 1/2 height, h, are calculated at the K-th element only. These functions $g_1(\phi)$ and $g_2(\phi)$ in Equation (1) are defined implicitly by the solution found by solving Equation (6) with the Ansys Fluent Solver [4].

Given the objective function below:

$$f(\phi) = G(P(\phi), \phi) \tag{9}$$

where f represents either of the two possible implicit constraints and is specified by a function G that depends directly on the design parameter and indirectly on ϕ via the nodal pressure vector P [4]. If the surface is sufficiently smooth, the adjoint variable approach can be used to determine how sensitive F is to changes in the design variable ϕ_i.

$$\frac{Df}{D\phi_i} = \frac{\partial G}{\partial \phi_i} - \lambda \cdot \frac{\partial R}{\partial \phi_i} \tag{10}$$

where the adjoint variable vector λ is calculated from the system of linear equations.

$$\left[\frac{\partial R}{\partial P}\right]^T \lambda = \left(\frac{\partial G}{\partial P}\right)^T \tag{11}$$

For the aforementioned performance metric, $\frac{\partial G}{\partial P}$ represents the adjoint load. The adjoint variable approach is computationally cost-effective because only one linear adjoint problem, defined by Equation (11), needs to be analyzed for each implicit objective and constraint function [4].

3.4. Adjoint Optimization Methodology

This part describes the approach taken to handle the uneven distribution of the melt along the width of the coat-hanger die. The coat-hanger die being examined is used by a nearby polypropylene sheet manufacturer and has dimensions provided in Table 1, as shown in Figure 1. It is specifically designed to produce 720 mm wide and 3 mm thick sheets.

Table 1. The quantitative parameters of the coat-hanger die.

Entrance Diameter (mm)	Distance between Inlet and Outlet (mm)	Thickness (mm)	Width (mm)	Gap Height (mm)	Gap Width (mm)
20	250	85	750	3	720

The process loop shown in Figure 2's flow chart outlines how to optimize the coat-hanger die using the adjoint method. The loop is repeated until the updated geometry fulfills the necessary specifications. To automate the simulation and avoid the manual actions, an example script written in Scheme language is provided in Appendix A. The subsequent sections will provide a detailed discussion of the steps involved in adjoint optimization.

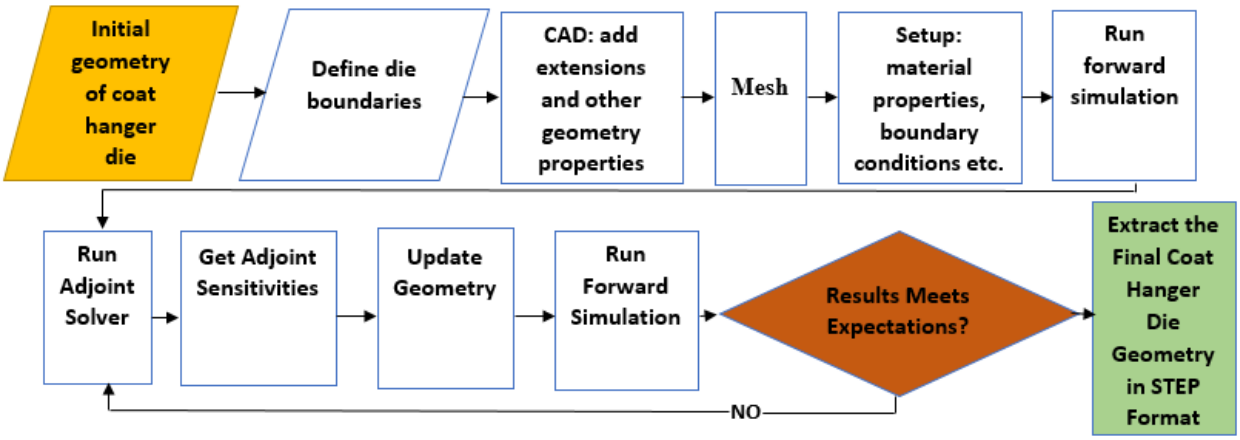

Figure 2. Flow chart of the adjoint optimization method.

3.4.1. Defining Boundary Conditions and Geometry of the Coat-Hanger Die

The boundaries of the coat-hanger die are defined as follows:

- Inlet: The flow is assumed to be fully developed with the volumetric flow rate of 8.5×10^{-5} m^3/s
- Wall: No-slip boundary condition
- Outlet: Zero normal and tangential forces.

Due to the symmetric nature of the coat-hanger die geometry only a quarter of the fluid domain of the coat-hanger die was used to reduce the computation time, as illustrated in Figure 1.

The present investigation employed a tetrahedron mesh composed of 972,007 cells with an element size of 1.0×10^{-3} m, accompanied by 5 inflation layers, as illustrated in Figure 3.

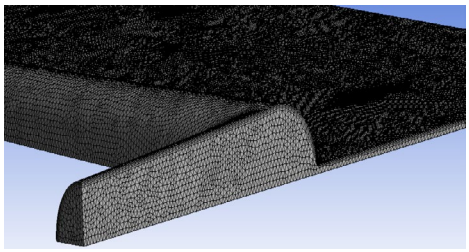

Figure 3. The fluid domain mesh.

3.4.2. Forward Simulation

Prior to running the adjoint solver, a forward simulation must be conducted to obtain the initial velocity values throughout the die body. The properties of the polypropylene material were given in the form of a Carreau–Yasuda viscosity model [34] as shown in Equation (12):

$$\eta = na\,\eta_\infty \alpha_T + \alpha_T(\eta_0 - \eta_\infty)\left(1 + \left(\lambda \alpha_T \dot{\gamma}\right)^a\right)^{\frac{n-1}{a}} \quad (12)$$

where, η_0—Zero shear viscosity (Pa · s), η_∞—Infinity shear viscosity (Pa · s), $\dot{\gamma}$—effective shear rate (s^{-1}), n—exponent (dimensionless), a—transition parameter (dimensionless), α_T—temperature dependence (dimensionless), λ—time constant (s).

The parameters for the Carreau-Yasuda viscosity model used in this study are shown in Table 2.

Table 2. List of parameters used in the simulation.

Parameter	Value
Zero-shear rate viscosity, η_0	8920 Pa · s
Time constant, λ	1.58 s
Power-law index, n	0.496
Index that controls the transition from the Newtonian plateau to the power-law region, α	2

After the first run of the fluid calculation from FLUENT, the obtained results for both pressure and velocity will be used to initialize the computation for the adjoint observable.

3.4.3. Standard Deviation

A standard deviation is a measurement of the data's variance from the mean.

The formula below is used to calculate the standard deviation of a given field variable on a surface:

$$\sqrt{\frac{\sum_{i=1}^{n}(x - x_0)^2}{n}} \quad (13)$$

And x_0 is given by:

$$x_0 = \frac{\sum_{i=1}^{n} x}{n} \quad (14)$$

3.4.4. Adjoint Solver

This research aims to achieve a uniform distribution of the melt across the width of the die. To accomplish this, the mass flux variance at the die outlet serves as the observable adjoint, which must be minimized. To determine the mass flux variance, one needs to calculate the surface integral of the mass flow rate across the die outlet.

To begin the optimization process with the adjoint solver, it was necessary to specify the desired reduction in the mass flux variance. The target reduction was initially set to 5% and applied in the first 60 iterations. However, towards the end of the computation

(from the 61st to 80th iterations), a 2% reduction was deemed more appropriate as the 5% reduction was too aggressive. Note that the percentage reduction depends on the choice of usage. In order to reduce simulation time, a 5% reduction was first chosen, and afterward, a 2% reduction.

Once the target change in the observable value has been established, the design change necessary to achieve a 5% or 2% reduction in mass flux variance must be calculated, and the mesh must be updated accordingly. The optimization process involved 80 iterations, with the first 50 iterations aimed at achieving a 5% reduction and the remaining 30 iterations focused on a 2% reduction in the observable value. As there is a repetitive loop between the first 50 and last 30 iterations, the script provided in Appendix A can be employed instead of running the optimization process manually 80 times.

Finally, the optimized geometry is extracted in an STL form using the Export STL button.

4. Results and Discussion

4.1. Mesh Independency Study

To ensure that accurate and reliable results were obtained in this study, the mesh independency study was performed to obtain the appropriate mesh size and density required. The mesh independency study was performed for the coat-hanger fluid domain starting with a mesh element of 50,000. From Figure 4, a mesh size of 500,000 and above found no variation in the maximum outlet velocity. Hence, we adopted a mesh size of 1.0×10^{-3} m having 972,007 elements.

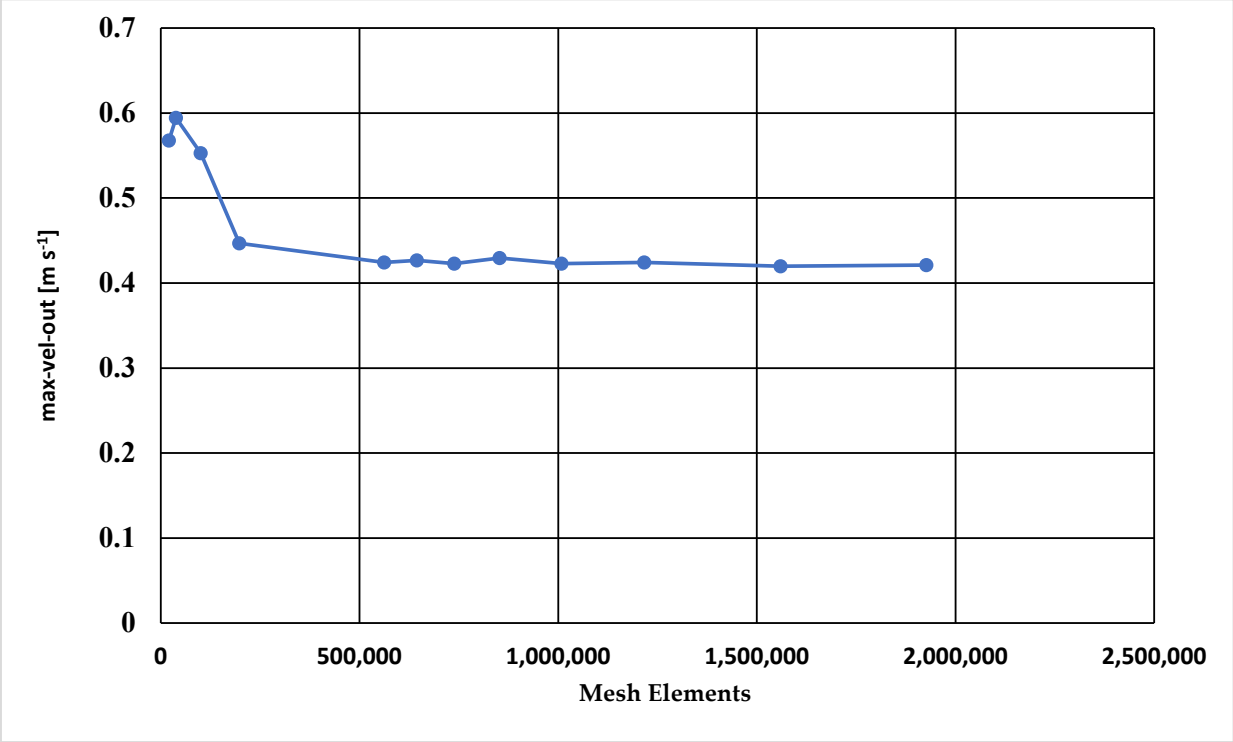

Figure 4. Mesh Independency Study.

4.2. Ansys Fluent and Adjoint Results

This section presents the optimization outcomes carried out using the adjoint solver. Figure 5a at the 0th iteration initially demonstrated that the outlet velocity was nearly 10 times higher at the die center than at the edges. Aggressive enhancement in the outlet velocity was noticeable from the 0th to 50th iteration (Figure 5a–e). From the 51st to 80th (Figure 5f–i) iteration, the improvement in the mass flux variance was smoother. Consequently, the outlet velocity became more uniform than the velocity distribution prior

to optimization. As shown in Figure 6, there was a reduction of 71.6% in the mass flux difference at the die outlet from 0.015069 kg m^{-2} s^{-1} to 0.004281 kg m^{-2} s^{-1}. Also, the improvement of the outlet velocity can be compared in terms of the standard deviation which was reduced from 0.097 to 0.015.

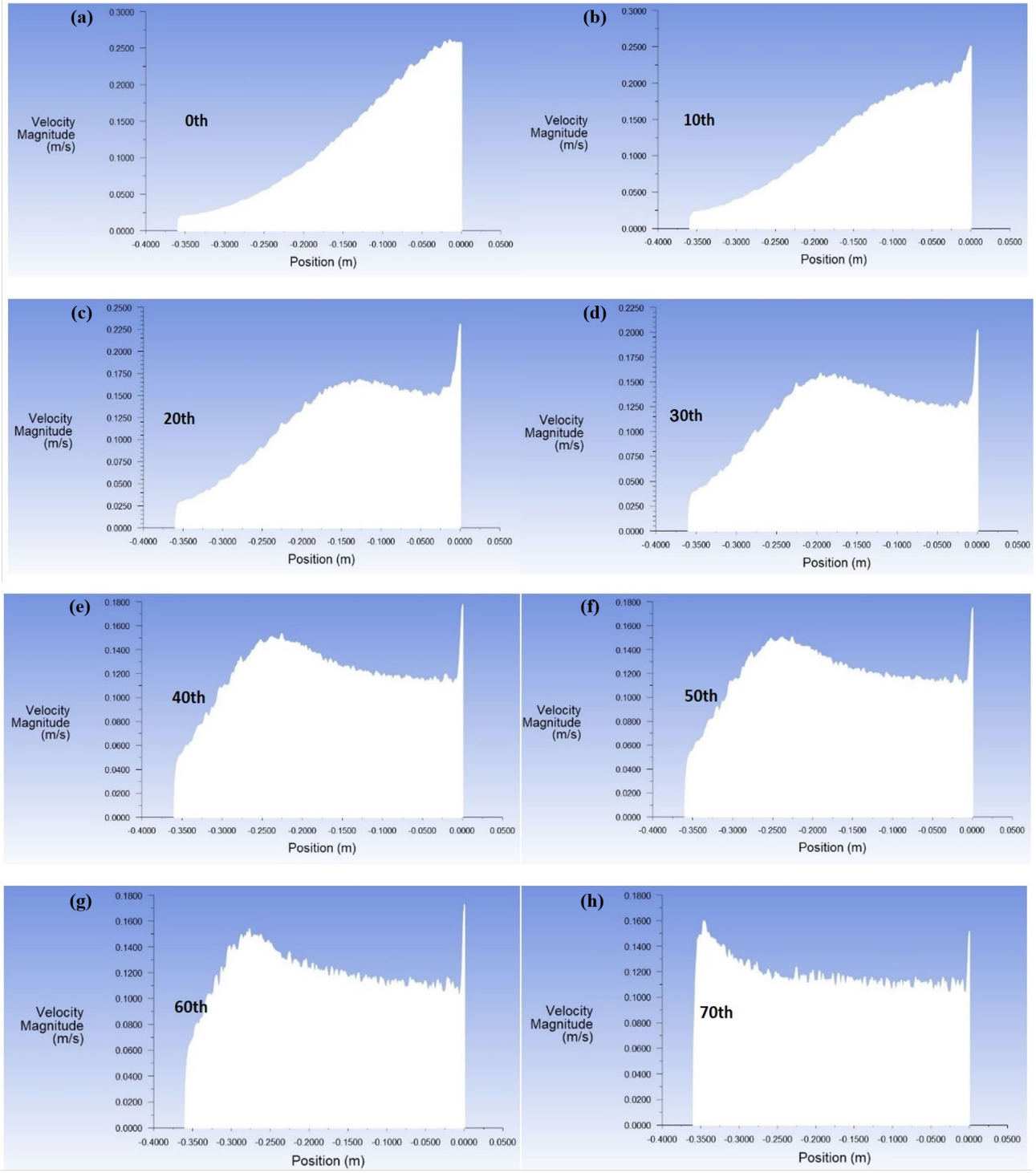

Figure 5. *Cont.*

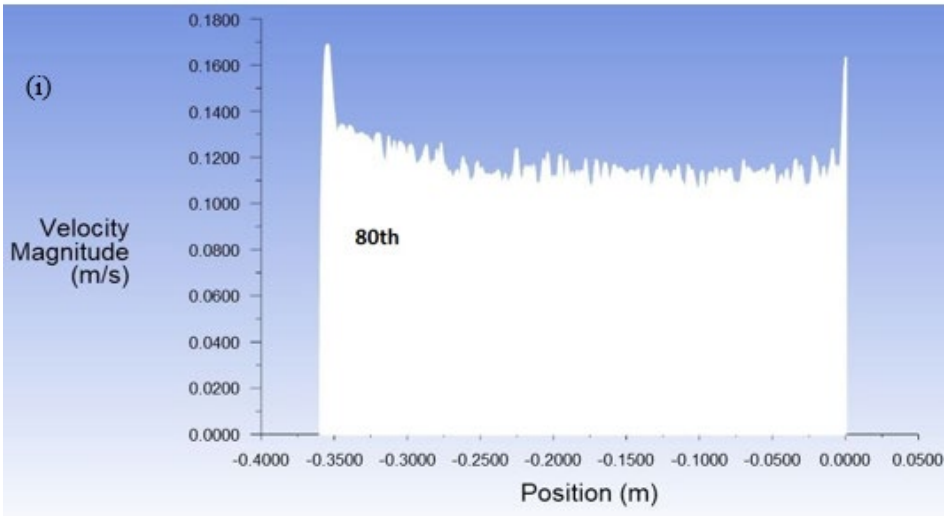

Figure 5. Outlet velocity plot: (**a**) 0th iteration, (**b**) 10th iteration, (**c**) 20th iteration, (**d**) 30th iteration, (**e**) 40th iteration, (**f**) 50th iteration, (**g**) 60th iteration, (**h**) 70th iteration, and (**i**) 80th iteration.

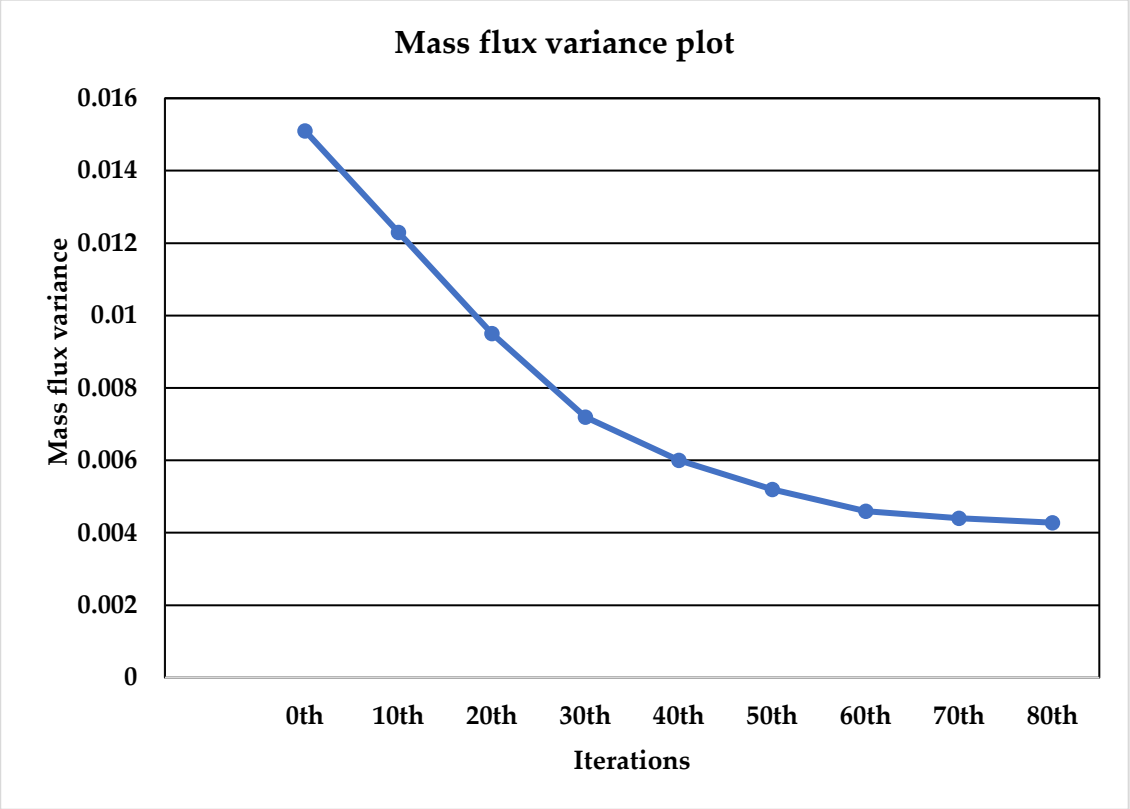

Figure 6. Mass flux variance minimization kg m^{-2} s^{-1}.

Figure 7 illustrates the improved velocity distribution across the die land after 80 iterations. Initially, during the 0th iteration (Figure 7a), the low-velocity region (ranging from 0 to 0.142 m/s) occupied one-third of the die from the edge. However, in the 80th iteration (Figure 7i), a uniform distribution was achieved across the land ranging from 0.172 m/s to 0.258 m/s. Nonetheless, there is a small region in the middle where the velocity ranges from 0.515 m/s to 0.061 m/s.

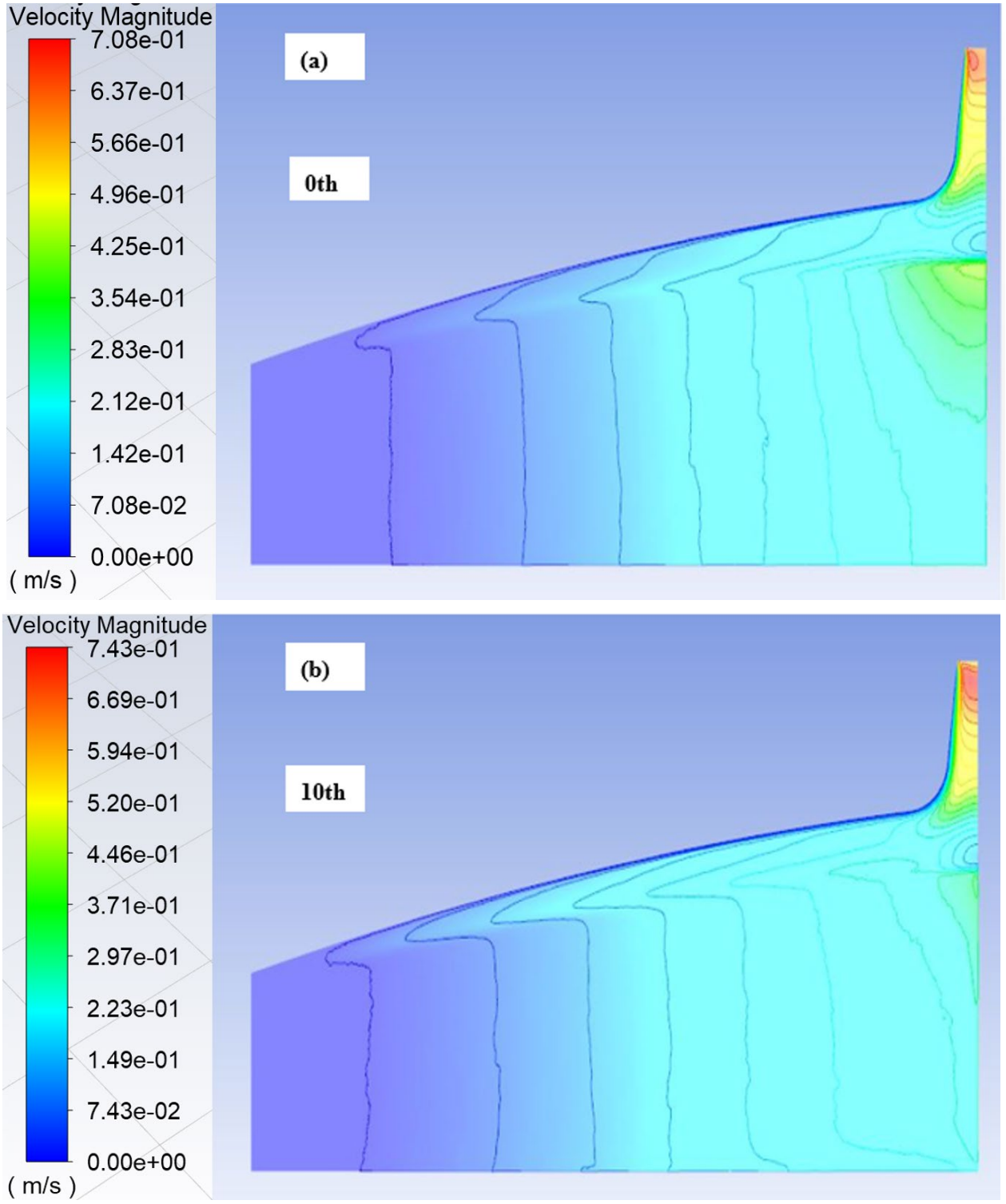

Figure 7. *Cont.*

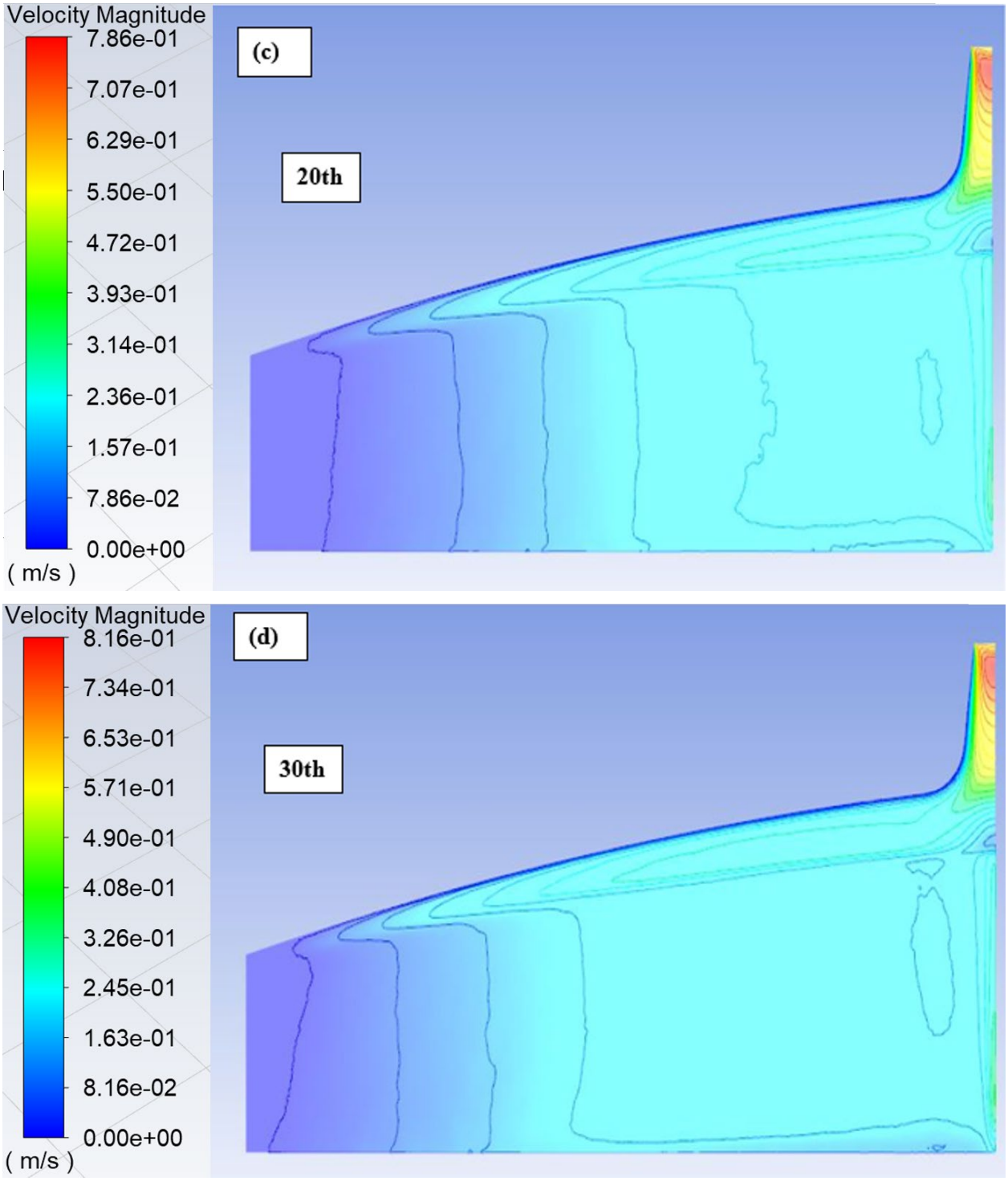

Figure 7. *Cont.*

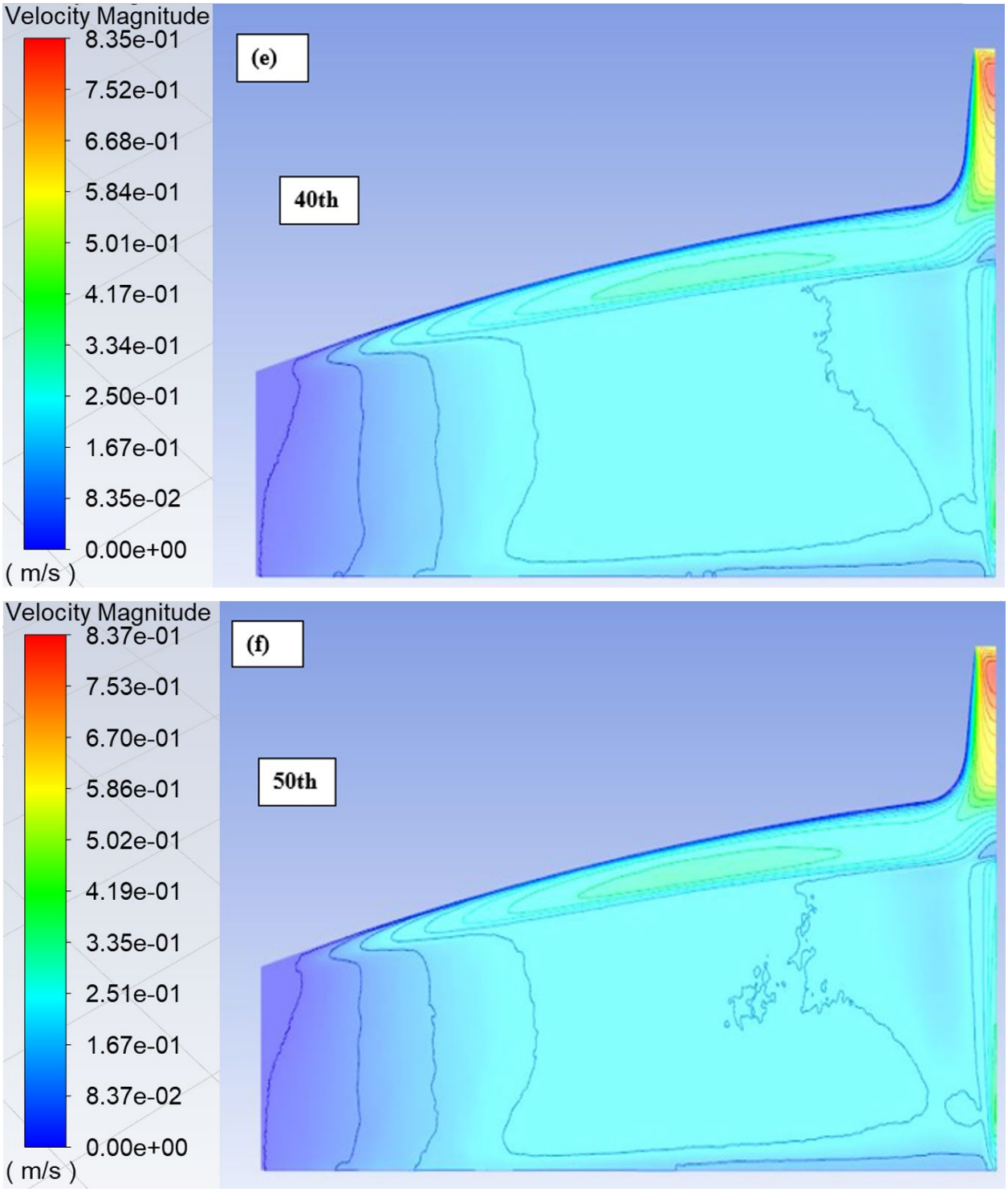

Figure 7. *Cont.*

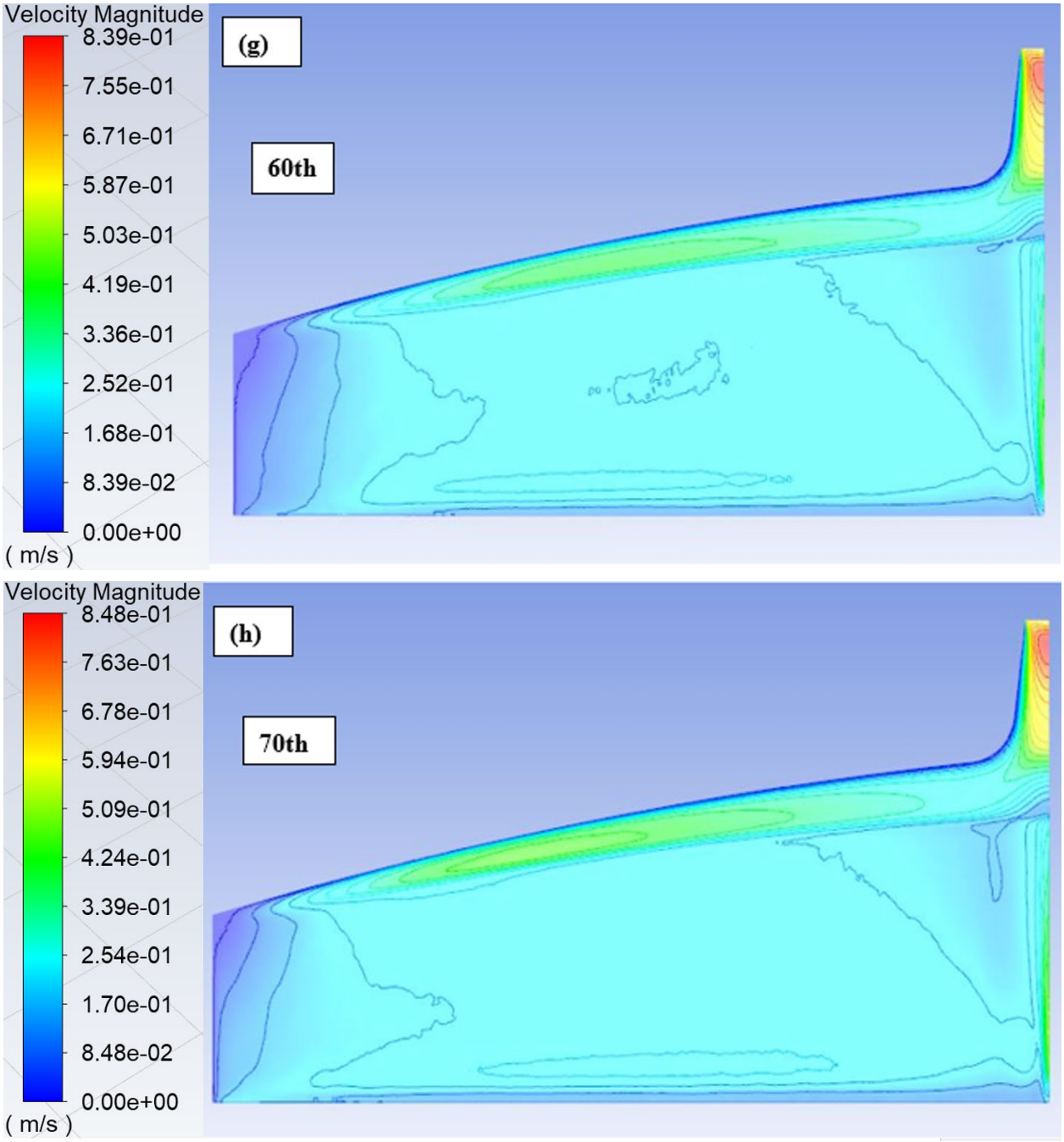

Figure 7. *Cont.*

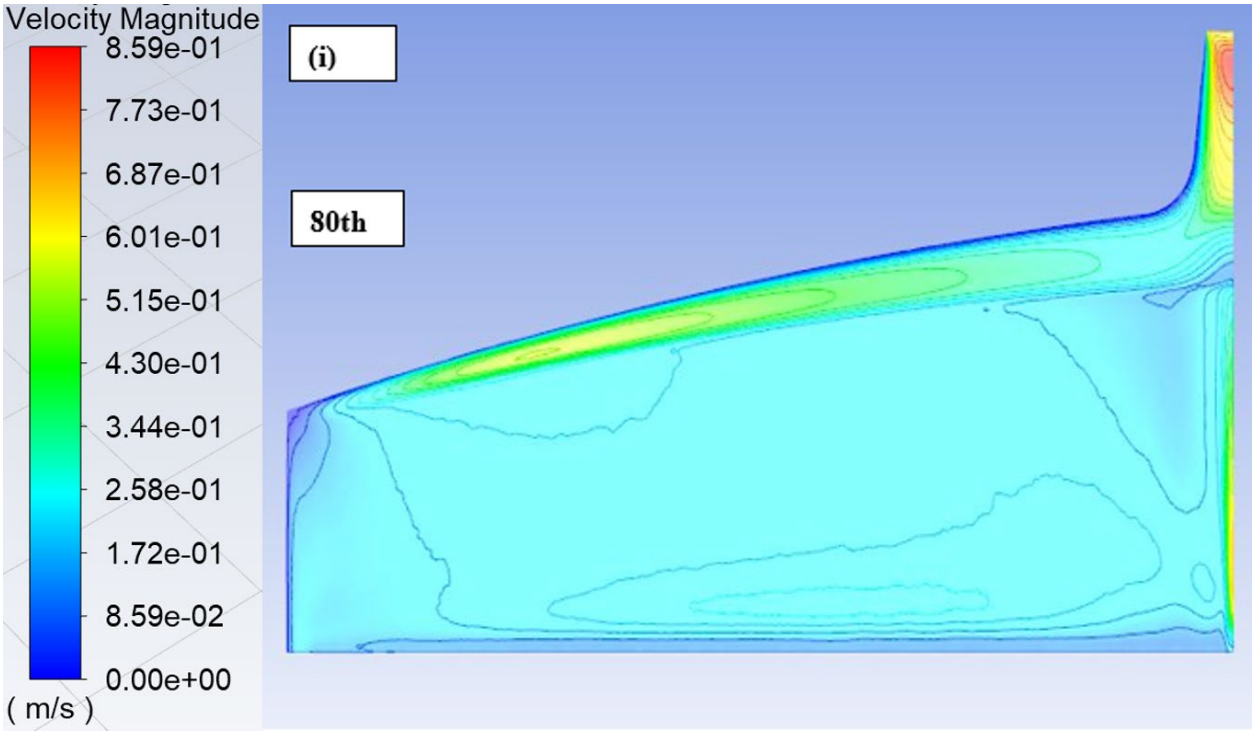

Figure 7. Velocity contour plots: (**a**) 0th iteration, (**b**) 10th iteration, (**c**) 20th iteration, (**d**) 30th iteration, (**e**) 40th iteration, (**f**) 50th iteration, (**g**) 60th iteration, (**h**) 70th iteration, and (**i**) 80th iteration.

In addition, the pressure distribution recorded in Figure 8 reveals that the difference between the inlet and outlet pressures results in the pressure drop value. Given that the inlet pressure is considerably greater than the outlet pressure, the pressure drop value is equivalent to the inlet pressure in our case. However, after 80 iterations, the pressure drop value remained unchanged as our target observation was solely the reduction in mass flux variance. Figure 8 depicts that the pressure drop value increased from 14.5 MPa to 16.5 MPa from the 0th (Figure 8a) to the 80th (Figure 8i) iteration, indicating that the improvements made to the coat-hanger die's flow uniformity did not yield favorable pressure results. This is because we only used mass flux variance as our observable during the simulation.

Lastly, Figure 9 compares the coat-hanger die geometry before and after optimization. The fluid domain volume increases against the number of iterations is plotted in Figure 10. The fluid domain's initial volume was estimated to be 91,703.07 mm^3, while after optimization, it increased to 93,116.98 mm^3. The fluid domain's volume increased due to the change in bounded regions during the optimization process. Upon observing the side views, it is evident that some regions of the fluid domain experienced a slight increase in volume, resulting in the thickening of the slit in those areas.

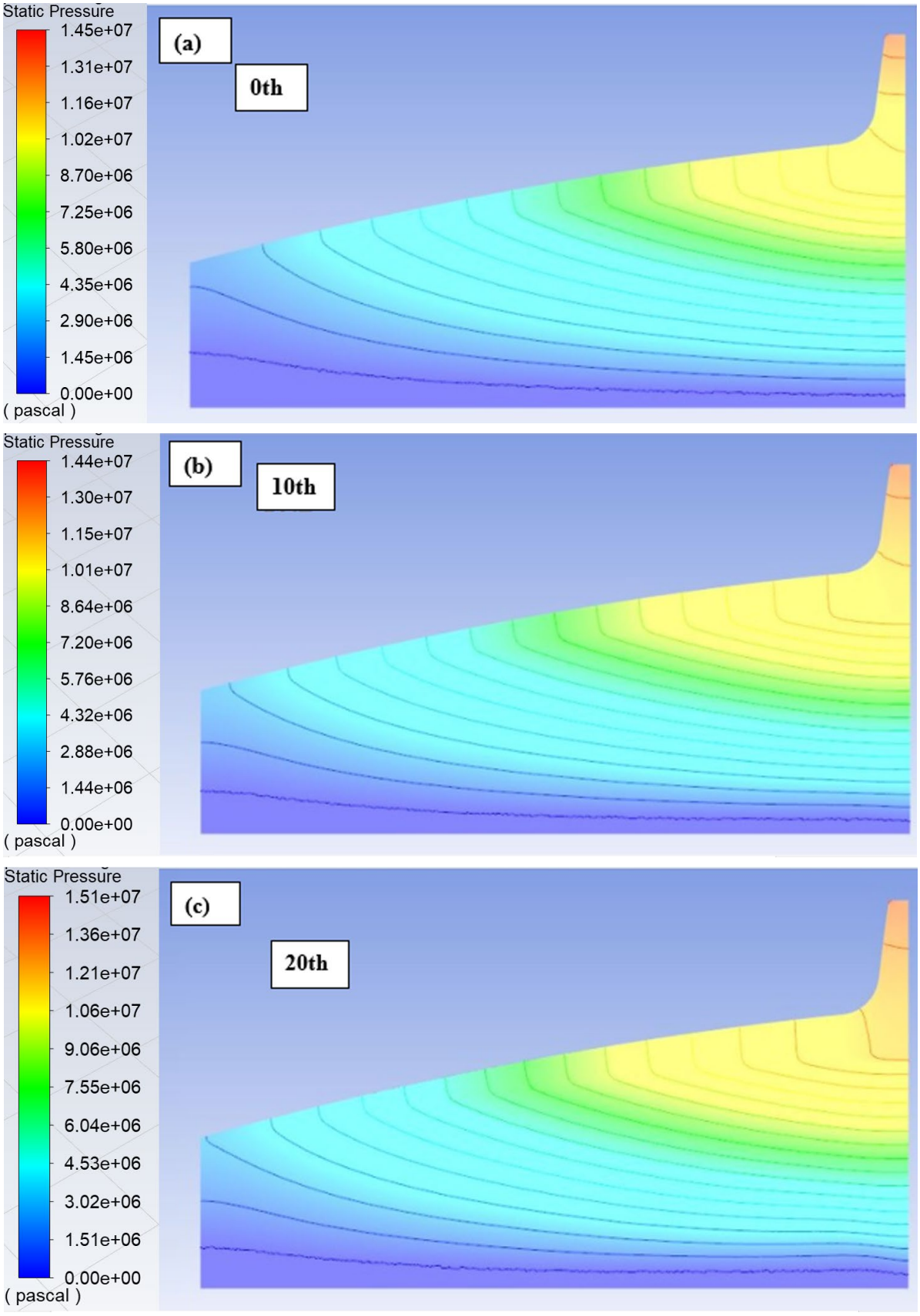

Figure 8. *Cont.*

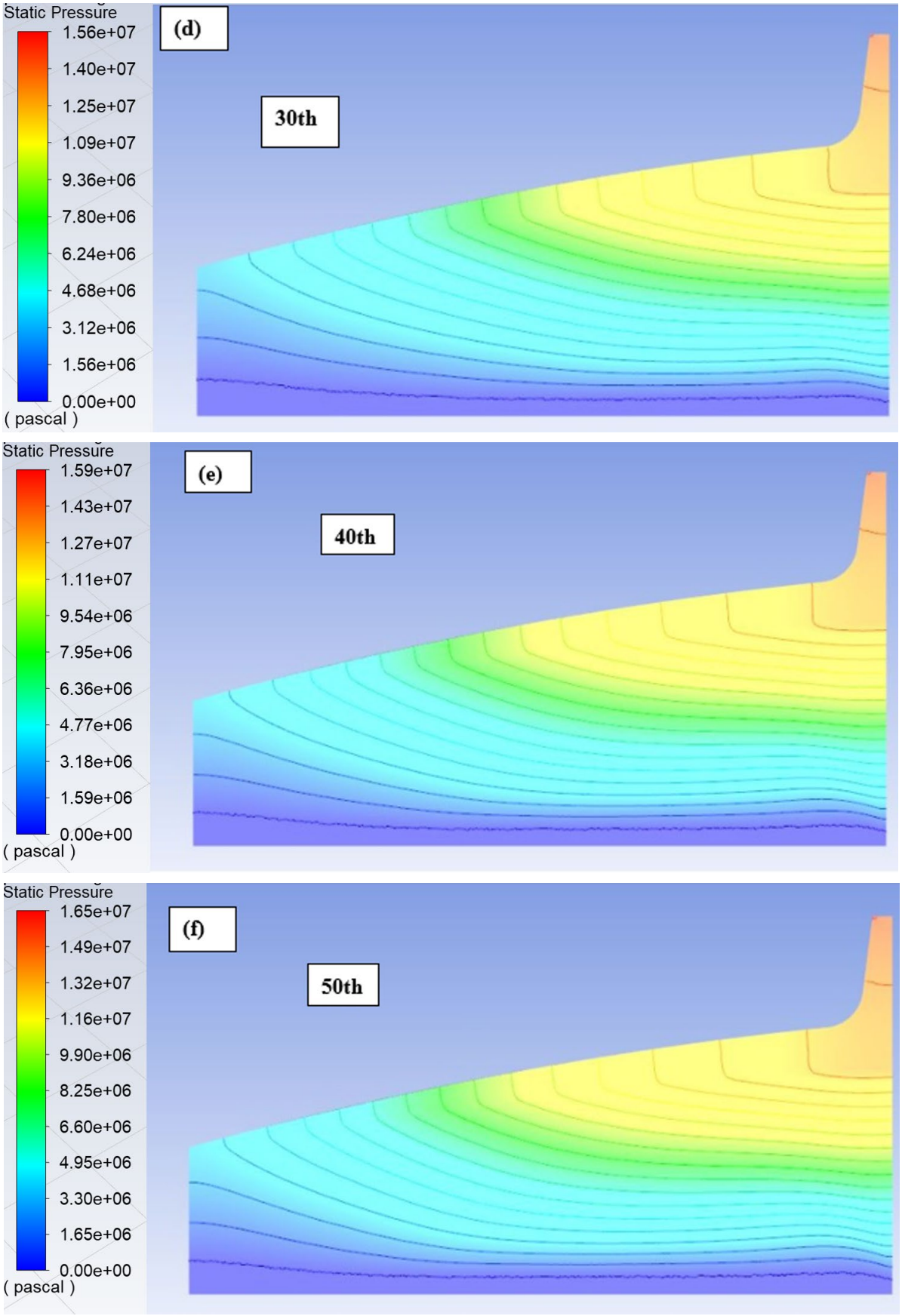

Figure 8. *Cont.*

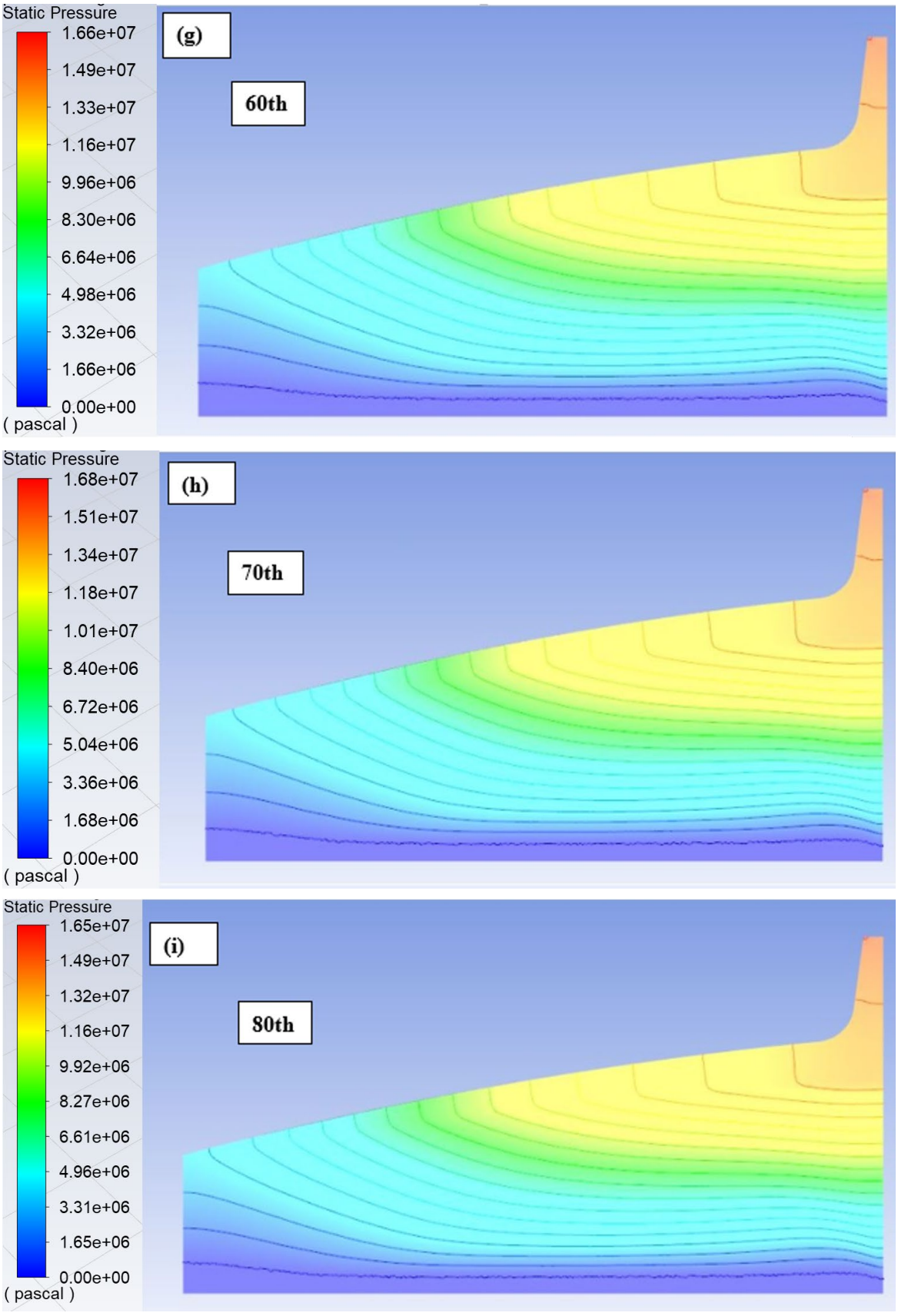

Figure 8. Pressure contour plots: (**a**) 0th iteration, (**b**) 10th iteration, (**c**) 20th iteration, (**d**) 30th iteration, (**e**) 40th iteration, (**f**) 50th iteration, (**g**) 60th iteration, (**h**) 70th iteration, and (**i**) 80th iteration.

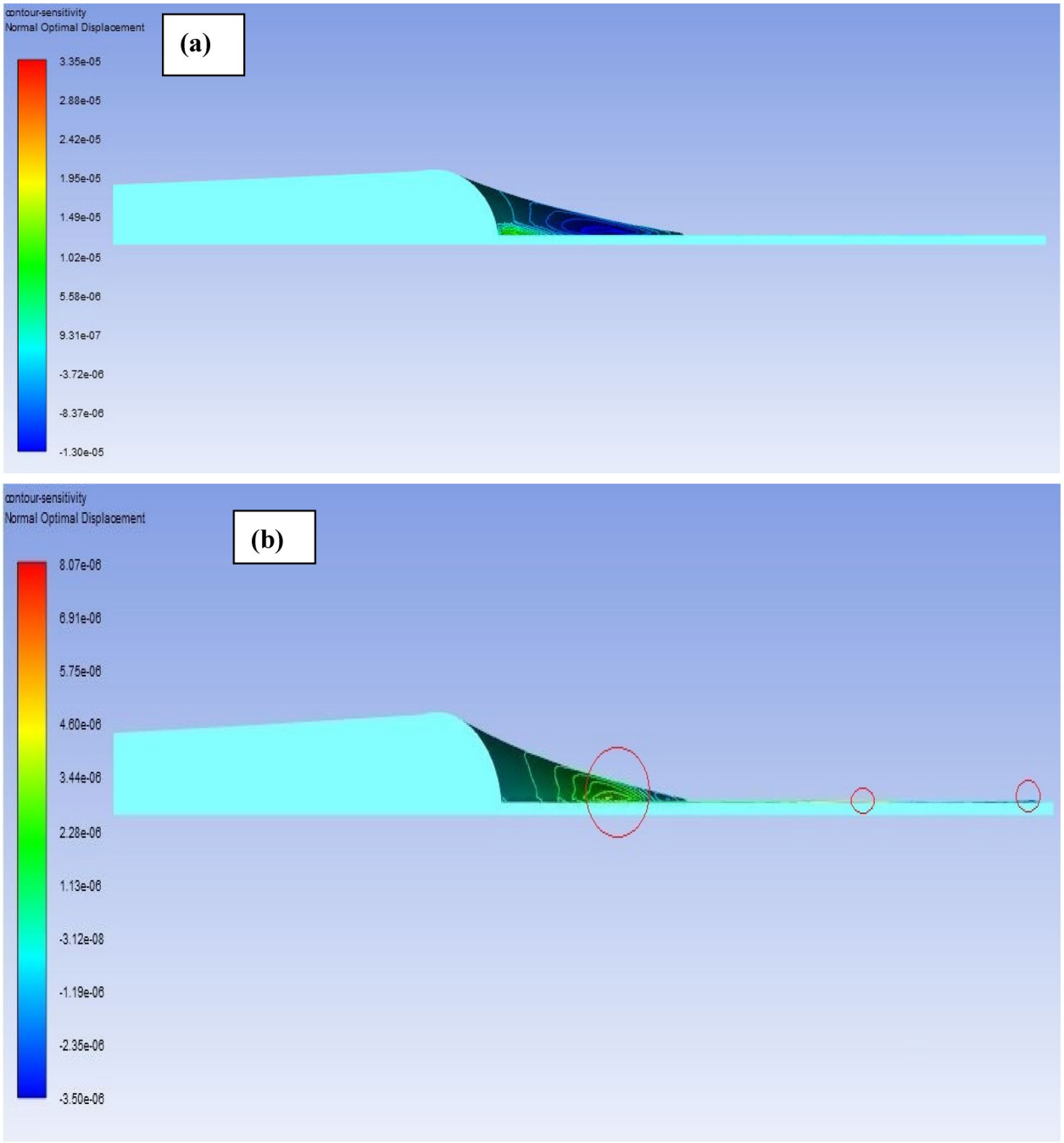

Figure 9. The geometry changes after the mesh modification/optimization: (**a**) 0th iteration and (**b**) 80th.

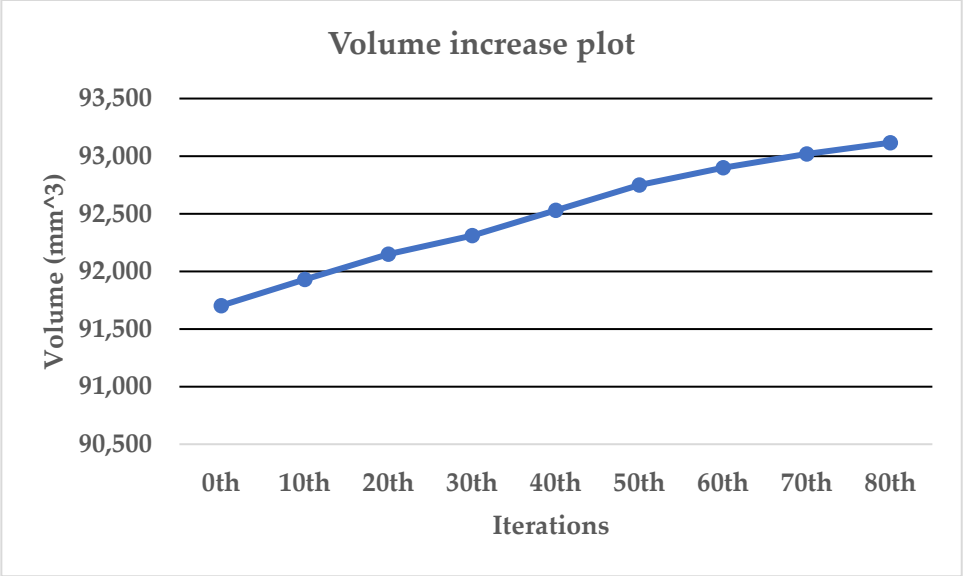

Figure 10. Fluid domain volume vs. number of iterations plot.

5. Conclusions

In conclusion, this paper aimed to enhance the uniform flow of the polymer melt through the coat-hanger die by utilizing the Adjoint Method. This research demonstrated the applicability of the adjoint solver in coat-hanger die design for non-Newtonian fluids, such as polymer melt. The resulting coat-hanger die geometry produced a more uniform melt flow, as evidenced by the velocity contour plot and outlet velocity graph across the die slit region. The variance in mass flow at the outlet of the die was considerably decreased by 71.6%, going from 0.015069 kg m^{-2} s^{-1} to 0.004281 kg m^{-2} s^{-1}. Additionally, the deviation in outlet velocity was reduced from 0.097 to 0.015. Therefore, the adjoint solver can be considered a powerful tool for optimizing coat-hanger dies for non-Newtonian fluids. However, concerns were raised regarding the computation time, which was approximately 26 h, and the feasibility of machining the geometry changes depicted in Figure 9. Also, future work will be based on the defined objective function in this paper whereby the pressure and velocity will be linearly combined as observables to obtain results for both pressure drop and uniform velocity at the die outlet.

In order to develop various syntaxes for different shape optimization objectives and residuals, familiarity with the scheme programming language syntax is required. It should be noted that the initial solution from the first iteration of the ANSYS Fluent solver is relied upon by the adjoint solver, which could lead to variations in results when different rheology models are used. With different rheology models used, there could be variations in results that were not accounted for in this study. As such, future research will delve into the extent of the variation in optimization for different rheological models.

Author Contributions: Conceptualization, A.P. and D.W.; methodology, D.I.; software, D.I. and O.C.; validation, D.I., O.C. and D.Z.; formal analysis, D.I. and O.C.; investigation, D.I. and O.C.; resources, A.P.; writing—original draft preparation, D.I. and O.C.; writing—review and editing, A.P., D.W. and D.Z.; supervision, D.W., A.P. and D.Z.; project administration, A.P.; funding acquisition, D.W. All authors have read and agreed to the published version of the manuscript.

Funding: This research was funded by Nazarbayev University under the Faculty Development Competitive Research Grant Program No. 021220FD4651, "Design & Development of Multiphysics Algorithm for Polymer Sheet Processing Die Design".

Data Availability Statement: All relevant data are contained within the article.

Conflicts of Interest: The authors declare no conflict of interest.

Nomenclature

P_{in}	inlet pressure
ϕ	design variables
F	objective function
h	height
g_1, g_2, g_3	constraints
$\overline{v}(\phi)$	mean velocity
$v_a(\phi)$	exit velocity
L	length
Q	flow rate
C_p	heat capacity at steady pressure
ρ	density
U	velocity
T	temperature
P	pressure
$\bigtriangledown$	gradient operator
Ω	cavity domain
S	conductance
R	residuals
x	cell value of selected variables at each facet
x_0	mean of x
n	total number of facets.

Appendix A

```
(define start_loop 1)
(define end_loop 60)
(define x start_loop)
(define max-iter-adjoint 20)

(do ((x start_loop (+ x 1))) ((> x end_loop))

(display x)

(ti-menu-load-string "/adjoint/run/initialize \n")
(ti-menu-load-string (format #f "/adjoint/run/iterate ~a \n" max-iter-adjoint))
(ti-menu-load-string "/adjoint/controls/stabilization yes 3 40 no\n")
(ti-menu-load-string "/adjoint/run/iterate 20 \n")

(ti-menu-load-string "/adjoint/design-tool/design-change/calculate-design-change \n")
(ti-menu-load-string "/adjoint/design-tool/design-change/modify-mesh \n")

(ti-menu-load-string "solve iterate,")


(ti-menu-load-string "/adjoint/observable/select \"mass-flux-variance\" no \n")
(ti-menu-load-string "/adjoint/observable/write yes observables.txt yes \n")

(ti-menu-load-string "/adjoint/observable/select \"mass-flux-variance\" no \n")
)
```

```
(define start_loop 1)
(define end_loop 60)
(define x start_loop)
(define max-iter-adjoint 20)

(do ((x start_loop (+ x 1))) ((> x end_loop))

    (display x)

    (ti-menu-load-string "/adjoint/run/initialize \n")
    (ti-menu-load-string (format #f "/adjoint/run/iterate ~a \n" max-iter-adjoint))
    (ti-menu-load-string "/adjoint/controls/stabilization yes 3 40 no\n")
    (ti-menu-load-string "/adjoint/run/iterate 20 \n")

    (ti-menu-load-string "/adjoint/design-tool/design-change/calculate-design-change \n")
    (ti-menu-load-string "/adjoint/design-tool/design-change/modify-mesh \n")

    (ti-menu-load-string "solve iterate,")


    (ti-menu-load-string "/adjoint/observable/select \"mass-flux-variance\" no \n")
    (ti-menu-load-string "/adjoint/observable/write yes observables.txt yes \n")

    (ti-menu-load-string "/adjoint/observable/select \"mass-flux-variance\" no \n")
)
```

References

1. Lebaal, N.; Schmidt, F.; Puissant, S. Optimizations of coat-hanger die, using constraint optimization algorithm and taguchi method. *AIP Conf. Proc.* **2007**, *908*, 537–544. [CrossRef]
2. Na, S.Y.; Do, H.K. *Three-Dimensional Simulation of Polymer Melt Flow in a Coat-Hanger Die*; Wiley: Hoboken, NJ, USA, 1996.
3. Han, W.; Wang, X. Optimal geometry design of the coat-hanger die with uniform outlet velocity and minimal residence time. *J. Appl. Polym. Sci.* **2012**, *123*, 2511–2516. [CrossRef]
4. Smith, D.E.; Wang, Q. Optimization-based design of polymer sheeting dies using generalized newtonian fluid models. *Polym. Eng. Sci.* **2005**, *45*, 953–965. [CrossRef]
5. Razeghiyadaki, A.; Zhang, D.; Wei, D.; Perveen, A. Optimization of polymer extrusion die based on response surface method. *Processes* **2020**, *8*, 1043. [CrossRef]
6. Lebaal, N.; Schmidt, F.; Puissant, S.; Lebaal, N.; Schmidt, F.; Design, S.P.; Lebaal, N.; Schmidt, F.; Puissant, S. Design and optimization of three-dimensional extrusion dies, using constraint optimization algorithm. *Finite Elem. Anal. Des.* **2019**, *45*, 333–340. [CrossRef]
7. Grieß, H.J.; Burghelea, T.I.; Münstedt, H. Velocity Measurements on a Polypropylene Melt During Extrusion Through a Flat Coat-Hanger Die. *Polym. Eng. Sci.* **2012**, *52*, 615–624. [CrossRef]
8. Igali, D.; Perveen, A.; Zhang, D.; Wei, D. Shear rate coat-hanger die using casson viscosity model. *Processes* **2020**, *8*, 1524. [CrossRef]
9. Pini, M.; Persico, G.; Pasquale, D.; Rebay, S. Adjoint method for shape optimization in real-gas flow applications. *J. Eng. Gas Turbines Power* **2015**, *137*, 032604. [CrossRef]
10. Othmer, C. Adjoint methods for car aerodynamics. *J. Math. Ind.* **2014**, *4*, 6. [CrossRef]
11. Razeghiyadaki, A.; Wei, D.; Perveen, A.; Zhang, D. A multi-rheology design method of sheeting polymer extrusion dies based on flow network and the winter-fritz design equation. *Polymers* **2021**, *13*, 1924. [CrossRef]
12. Razeghiyadaki, A.; Wei, D.; Perveen, A.; Zhang, D.; Wang, Y. Effects of Melt Temperature and Non-Isothermal Flow in Design of Coat Hanger Dies Based on Flow Network of Non-Newtonian Fluids. *Polymers* **2022**, *14*, 3161. [CrossRef] [PubMed]
13. Papoutsis-Kiachagias, E.M.; Magoulas, N.; Mueller, J.; Othmer, C.; Giannakoglou, K.C. Noise reduction in car aerodynamics using a surrogate objective function and the continuous adjoint method with wall functions. *Comput. Fluids* **2015**, *122*, 223–232. [CrossRef]
14. Giles, M.B.; Pierce, N.A. An introduction to the adjoint approach to design. *Flow Turbul. Combust.* **2000**, *65*, 393–415. [CrossRef]
15. Alonso, J.J. A Crash-Course on the Adjoint Method for Aerodynamic Shape Optimization. In Proceedings of the COBEM2003, the 17th International Congress of Mechanical Engineering, São Paulo, Brasil, 10–14 November 2003. Available online: http://citeseerx.ist.psu.edu/viewdoc/summary?doi=10.1.1.13.6065 (accessed on 1 March 2023).
16. Jameson, A.; Alonso, J.; Reuther, J.; Martinelli, L.; Vassberg, J. Aerodynamic shape optimization techniques based on control theory. In *Computational Mathematics Driven by Industrial Problems*; Springer: Berlin/Heidelberg, Germany, 1998. [CrossRef]

17. Nielsen, E.J.; Anderson, W.K. Recent improvements in aerodynamic design optimization on unstructured meshes. *AIAA J.* **2001**, *40*. [CrossRef]
18. Elliott, J.; Peraire, J. Practical 3d aerodynamic design and optimization using unstructured meshes. *AIAA J.* **1996**, *35*, 1819–1828. [CrossRef]
19. Soto, O.; Löhner, R.; Yang, C. An adjoint-based design methodology for CFD problems. *Int. J. Numer. Methods Heat Fluid Flow* **2004**, *14*, 734–759. [CrossRef]
20. Smith, D.E.; Wang, Q. An optimization-based approach to compute sheeting die designs for multiple operating conditions. *Polym. Eng. Sci.* **2004**, *6*, 4741–4751.
21. Pujos, C.; Regnier, N.; Mousseau, P.; Defaye, G.; Jarny, Y. Estimation of rheological law by inverse method from flow and temperature measurements with an extrusion die. *AIP Conf. Proc.* **2007**, *908*, 1287–1294. [CrossRef]
22. Pujos, C.; Régnier, N.; Defaye, G. Determination of the inlet temperature profile of an extrusion die in unsteady flow. *Chem. Eng. Process. Process Intensif.* **2008**, *47*, 456–462. [CrossRef]
23. Zeng, T.; Jewkes, J.; Abo-serie, E. Conformal Cooling Channel Shape Optimisation for High-Pressure Aluminium Die-Casting Tools Using the Adjoint Method. In Proceedings of the 17th UK Heat Transfer Conference (UKHTC2021), Manchester, UK, 4–6 April 2022.
24. Smith, D.E. Design sensitivity analysis and optimization for polymer sheet extrusion and mold filling processes. *Int. J. Numer. Methods Eng.* **2003**, *57*, 1381–1411. [CrossRef]
25. Smith, D.E.; Tortorelli, D.A.; Tucker, C.L. Optimal design for polymer extrusion. Part II: Sensitivity analysis for weakly-coupled nonlinear steady-state systems. *Comput. Methods Appl. Mech. Eng.* **1998**, *167*, 303–323. [CrossRef]
26. Smith, D.E.; Tortorelli, D.A.; Tucker, C.L. Optimal design and analysis for polymer extrusion and molding. In Proceedings of the 6th Symposium on Multidisciplinary Analysis and Optimization, Bellevue, WA, USA, 4–6 September 1996; pp. 1019–1024. [CrossRef]
27. Smith, D.E.; Tortorelli, D.A.; Tucker, C.L. Optimal design for polymer extrusion. Part I: Sensitivity analysis for nonlinear steady-state systems. *Comput. Methods Appl. Mech. Eng.* **1998**, *167*, 283–302. [CrossRef]
28. Giles, M.B.; Duta, M.C.; Müller, J.D.; Pierce, N.A. Algorithm developments for discrete adjoint methods. *AIAA J.* **2003**, *41*, 198–205. [CrossRef]
29. Li, S.; Petzold, L. Adjoint sensitivity analysis for time-dependent partial differential equations with adaptive mesh refinement. *J. Comput. Phys.* **2004**, *198*, 310–325. [CrossRef]
30. Mavriplis, D.J. Discrete adjoint-based approach for optimization problems on three-dimensional unstructured meshes. *AIAA J.* **2007**, *45*, 740–750. [CrossRef]
31. Thomas, J.P.; Hall, K.C.; Dowell, E.H. A discrete adjoint approach for modeling unsteady aerodynamic design sensitivities. In Proceedings of the 41st Aerospace Sciences Meeting and Exhibit, Reno, Nevada, 6–9 January 2003; Volume 43. [CrossRef]
32. Dybvig, R.K. *The Scheme Programming Language*; MIT Press: Cambridge, MA, USA, 2009; ISBN 9780262512985.
33. Aror, J.S. *Introduction to Optimum Design*, 3rd ed.; Academic Press: Cambridge, MA, USA, 2011; ISBN 9780123813756.
34. Han, W.; Wang, X. Optimal geometry design of the coat-hanger die used for melt blown nonwoven processing. *Adv. Mater. Res.* **2011**, *331*, 444–448. [CrossRef]

Disclaimer/Publisher's Note: The statements, opinions and data contained in all publications are solely those of the individual author(s) and contributor(s) and not of MDPI and/or the editor(s). MDPI and/or the editor(s) disclaim responsibility for any injury to people or property resulting from any ideas, methods, instructions or products referred to in the content.